Geometry outside of acoustic black holes in (2 + 1)-dimensional spacetime

Qing-Bing Wang[1] and Xian-Hui Ge[1,2,*]

[1]*Department of Physics, Shanghai University, Shanghai 200444, China*
[2]*Center for Gravitation and Cosmology, College of Physical Science and Technology,*
Yangzhou University, Yangzhou 225009, China

Analogue black holes, which can mimic the kinetic aspects of real black holes, have been proposed for many years. The growth of the radial momentum toward the acoustic horizon is calculated for acoustic black holes in flat and curved spacetimes. Surprisingly, for a freely infalling vortex approaching the acoustic black hole, the Lyapunov exponent of the growth of the momentum at the horizon saturates the chaos bound $\Lambda_{\text{Lyapunov}} \leq 2\pi T$. We investigate the orbits of test vortices and sound wave rays in the (2 + 1)-dimensional "curved" spacetime of an acoustic black hole. We show that the vortices orbit, the sound wave orbit, and the time delay of sound are similar to those famous effects of general relativity. These effects can be verified experimentally in future experiments.

I. INTRODUCTION

Analogue black holes have recently been a hot topic as they can provide interesting connections between astrophysical phenomena with tabletop experiments. Remarkably, the very recent experiments have reported that the thermal Hawking radiation and the corresponding temperature were observed in a Bose-Einstein condensate system [1] (see [2] for the experiment on stimulated the Hawking radiation in an optical system). In the seminal paper of Unruh [3], the idea of using hydrodynamical flows as analogous systems to mimic a few properties of black hole physics was proposed. In this model, sound waves like light waves, cannot escape from the horizon, and therefore it is named "acoustic (sonic) black hole" (ABH). A moving fluid with speed exceeding the local sound velocity through a spherical surface could in principle form an acoustic black hole. The event horizon is located on the boundary between subsonic and supersonic flow regions. The horizon, ergosphere, and Hawking radiation of (3 + 1)-dimensional static and rotating acoustic black holes were later studied in [4]. The spherical singular hypersurface in static superfluid was studied in [5]. It was shown that these shells form acoustic lenses analog to the ordinary optical lenses.

Acoustic black holes for relativistic fluids were derived from the Abelian Higgs model [6–9]. Since the Abelian Higgs model describes high energy physics, the result in [8] implies that acoustic black holes might be created in high energy physical processes, such as quark matters and neutron stars. The quasi-one-dimensional supersonic flow of a Bose Einstein condensate (BEC) in Laval nozzle (convergent divergent nozzle) is considered in [10] in order to find out which experimental settings can amplify the effect of acoustic Hawking radiation and provide observable signals. The acoustic black holes with non-extremal black D3-brane were considered in [11]. The particle production near the horizon of the acoustic black hole was studied by [12]. The acoustic black hole geometry in a viscous fluid with a dissipation effect was considered in [13].

Recently, measures of operator complexity have received considerable attention in studies of information scrambling and quantum complexity in holographic systems [14,15]. The conjectured momentum/complexity duality states that the rate of operator complexity growth corresponds to appropriately defined radial component of momentum for a test system falling into a black hole [14,15]. For the Schwarzschild-AdS black hole, a test particle's momentum grows at a maximal rate [14] and the Lyapunov exponent obtained saturates the chaos bound $\Lambda_{\text{Lyapunov}} \leq 2\pi T$ proposed in [16]. It seems to be a universal property because all the near horizon regions with a nonzero temperature are locally the Rindler-like. We are going to examine the momentum growth of an infalling vortex toward acoustic black holes and check whether the chaos bound is saturated for analogue black holes. This might be realizable because acoustic black holes would be realized in tabletop experiments.

*Corresponding author.
gexh@shu.edu.cn

More than that, we further explore the geodesic motion outside a $(2 + 1)$-dimensional acoustic black hole. We will concentrate on predicting the orbits of "test" particles (i.e., vortices) in fluids and sound rays in the "curved" acoustic spacetime. We will exhibit the Lyapunov exponent of a particle falling radially near the event horizon and some well-known effects analogous to those in general relativity—the vortices orbits, the sound wave ray deflection, the time delay of sound waves for acoustic black holes. These results can be verified by two-dimensional spherically symmetric superfluid experiments.

The paper is organized as follows: In Sec. II, we briefly review the geometry of acoustic black holes. In Sec. III, considering an infalling vortex towards acoustic black holes, we calculate the growth of the radial momentum. In Sec. IV, we further consider the Lyapunov exponent of radial motion of vortices toward the event horizon of the acoustic black hole which is embedded in the Schwarzschild-anti–de Sitter (AdS) geometry. We then study the orbit of vortices and the corresponding stability in Sec. V. The sound wave trajectory is then studied in Sec. VI in which the deflection and the time delay of the sound wave prorogation are studied. The conclusion and discussions are provided in the last section.

II. THE METRIC OF ACOUSTIC BLACK HOLES IN FLAT AND CURVED SPACETIMES

In this section, we mainly consider three different kinds of acoustic black holes: the line element first given by Unruh [3,4], the metric obtained from the Gross-Pitaeskii equation in curved spacetime [6] and the metric obtained from general relativistic fluids [17–19]. The reason to consider these three different types of metric is for the purpose of examining the universality of the relation $\Lambda_{\text{Lyapunov}} \leq 2\pi T$. Later, we will focus on the geodesic motion in acoustic black hole in flat spacetime which is more realizable in experiments.

A. Acoustic black holes in Minkowski spacetime

We first consider the general acoustic black hole metric given by Unruh, which is derived from the fluid continuity equation in a uniform fluid medium [3] (see also [4]),

$$ds^2 = g_{tt}dt^2 + g_{rr}dr^2 + g_{\theta\theta}d\theta^2 + g_{\phi\phi}d\phi^2$$
$$= \frac{\rho_0}{c_s}\left[-(c_s^2 - v^2)dt^2 + \frac{c_s^2}{c_s^2 - v^2}dr^2 \right.$$
$$\left. + r^2(d\theta^2 + \sin^2\theta d\phi^2)\right]. \quad (1)$$

Here we assume the flow is a static spherically symmetric conservation flow. In this formula, c_s refers to the speed of sound in the fluid medium, and ρ_0 is the fluid density. The velocity v is the flow rate of the fluid along the radial

direction. Assuming ρ_0 and c_s are two constants and coordinates independent, absorbing the factor $\frac{\rho_0}{c_s}$ into the line element on the left and setting $c_s = 1$, we can write

$$ds^2 = -(1 - v^2)dt^2 + (1 - v^2)^{-1}dr^2$$
$$+ r^2(d\theta^2 + \sin^2\theta d\phi^2).$$

For a spatially two-dimensional fluid model, we can take $\theta = \frac{\pi}{2}$, so that $d\theta^2 = 0$, $\sin^2\theta = 1$. The metric rewritten in a matrix form is

$$g_{\mu\nu} = \begin{pmatrix} -(1 - v^2) & 0 & 0 \\ 0 & (1 - v^2)^{-1} & 0 \\ 0 & 0 & r^2 \end{pmatrix}. \quad (2)$$

It is also known from fluid continuity and incompressibility $\nabla \cdot \boldsymbol{v} = 0$ (for outside the central area), the speed v should satisfy $v = -\lambda/r$, where λ is a positive constant and the negative sign means that the direction of the fluid velocity points to the center of the acoustic black hole (see Fig. 1). Then the $(2 + 1)$-dimensional acoustic black hole metric can be written as [14,20]

$$ds^2 = -f(r)dt^2 + \frac{1}{f(r)}dr^2 + r^2d\phi^2,$$
$$f(r) = 1 - \frac{\lambda^2}{r^2}. \quad (3)$$

The acoustic event horizon locates at $r_0 = \lambda$. The Hawking temperature of the acoustic black hole is given by [3,4,21]

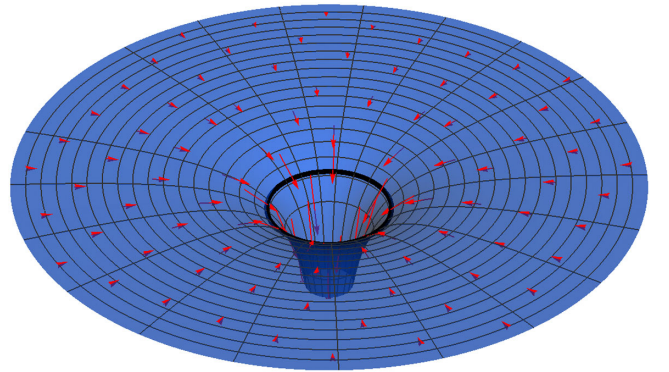$$T = \frac{f'(r)|_{r=\lambda}}{4\pi} = \frac{1}{2\pi\lambda}. \quad (4)$$

FIG. 1. Schematic view of a two-dimensional acoustic black hole. The arrow represents the direction of fluid flow. The black circle is the acoustic horizon where the fluid velocity reaches the sound velocity. The region in the ring represents the acoustic black hole. For the region in the central black circle, we can regard it as a sink leading to the high-dimensional space from which the fluid flows to the third dimensional space.

B. Acoustic black holes from Gross-Pitaeskii equation in curved spacetime

In curved spacetime, the Gross-Pitaeskii theory is given by

$$S = \int d^4x\sqrt{-g}\left(|\partial_\mu\varphi|^2 + m^2|\varphi|^2 - \frac{b}{2}|\varphi|^4\right), \quad (5)$$

where φ is a complex scalar order parameter. The function φ is taken as a probe and does not backreact on the background geometry. The acoustic black hole metric can be derived by considering perturbations around the background (ρ_0, θ_0): $\rho = \rho_0 + \rho_1$ and $\theta = \theta_0 + \theta_1$. The acoustic black hole metric then can be written as [6]

$$ds^2 = (g_{\mu\nu}^{GR} * g_{\mu\nu}^{ABH})dx^\mu dx^\nu$$
$$= \frac{c_s}{\sqrt{c_s^2 - v_\mu v^\mu}}\left[(c_s^2 - v_r v^r)g_{tt}^{GR}dt^2\right.$$
$$+ c_s^2\frac{c_s^2 - v_\mu v^\mu}{c_s^2 - v_r v^r}g_{rr}^{GR}dr^2 + (c_s^2 - v_\mu v^\mu)g_{\vartheta\vartheta}^{GR}d\vartheta^2$$
$$+ \left. g_{\phi\phi}^{GR}(c_s^2 - v_\mu v^\mu)d\phi^2\right], \quad (6)$$

where $v_t = -\dot{\theta}$, $v_i = \partial_i\theta$, $(i = r, \theta, \phi)$, c_s the sound of speed, m denotes a parameter related to the particle mass and b is a parameter. Intriguingly, this is an analogue black hole embedded in the spacetime governed by general relativity. Among them, $g_{\mu\nu}^{GR}$ is the spacetime metric of gravity and $g_{\mu\nu}^{ABH}$ describes the geometry of the acoustic black hole, where $\mu, \nu = t, r, \theta, \phi$. The metric tensor used to raise or lower indices of v_μ is by $g_{\mu\nu}^{GR}$. The dispersion relation is given by $v^\mu v_\mu = m^2 - c_s^2$. As $m = 0$, we can recover the normalized four-velocity relation $v^\mu v_\mu = -c_s^2$. For a Schwarzschild black hole in the background of thermal radiation, the event horizon is at $r_0 = 2M/c^2$. At $r_s = 6M/c^2$, the sound speed of thermal radiation is $c_s = c/\sqrt{3}$ with c the speed of light. In the region of $r < r_s$, the thermal radiation sound wave cannot escape, that is, r_s corresponds to the acoustic horizon.

As a warm-up exercise, we consider some kinds of fluid surrounded black holes in $(2 + 1)$-dimensional AdS space. In the following, we set $d\theta = 0$. The $(2 + 1)$-dimensional spacetime metric of AdS-Schwarzschild black holes is given by [22]

$$ds_{GR}^2 = -r^2\left(1 - \frac{r_0^2}{r^2}\right)dt^2 + \frac{1}{r^2(1 - \frac{r_0^2}{r^2})}dr^2 + r^2d\phi^2, \quad (7)$$

where r_0 is the radius of the black hole horizon, and we take AdS radius to be 1 and $G = M = c = 1$. Combined with the acoustic metric given in Eq. (1), we write down the

$(2 + 1)$-dimensional acoustic black hole metric embedded in AdS-Schwarzschild spacetime as follows:

$$ds^2 = (g_{\mu\nu}^{GR} * g_{\mu\nu}^{ABH})dx^\mu dx^\nu = \mathcal{G}_{tt}dt^2 + \mathcal{G}_{rr}dr^2 + \mathcal{G}_{\phi\phi}d\phi^2. \quad (8)$$

By setting $c^2 = 1$ and $c_s^2 = 1/3$ and taking the sign of $g_{\mu\nu}^{GR}$ as $\eta_{\mu\nu}$ and the sign of $g_{\mu\nu}^{ABH}$ as $\delta_{\mu\nu}$, we can write the metric components as

$$\mathcal{G}_{tt} = -\frac{1}{3}f_{ABH}(r)f_{GR}(r),$$
$$\mathcal{G}_{rr} = \frac{1}{f_{ABH}(r)f_{GR}(r)}, \qquad \mathcal{G}_{\phi\phi} = r^4, \quad (9)$$

where the blacken factors are given by

$$f_{ABH}(r) = 1 - \frac{3\lambda^2}{r^2}, \qquad f_{GR}(r) = r^2\left(1 - \frac{r_0^2}{r^2}\right). \quad (10)$$

Note that the horizon $\sqrt{3}\lambda$ of the acoustic black hole is required to be larger than the event horizon r_0 of the black hole. Inside the event horizon $\mathcal{G}_{tt}$ is less than 0 and $\mathcal{G}_{rr}$ is greater than 0; between the two horizons, i.e., $\sqrt{3}\lambda > r > r_0$, the opposite is true, $\mathcal{G}_{tt} > 0$ and $\mathcal{G}_{rr} < 0$.

In the curved spacetime, the Hawking temperature at the acoustic horizon is [6]

$$T = \frac{1}{4\pi\sqrt{\mathcal{G}_{rr}}}\left(-\sqrt{\frac{g_{tt}^{ABH}}{-g_{tt}^{GR}}}g_{tt}'^{GR} + \sqrt{\frac{-g_{tt}^{GR}}{g_{tt}^{ABH}}}g_{tt}'^{ABH}\right)\Bigg|_{r=\sqrt{3}\lambda}$$
$$= \frac{3\lambda^2 - r_0^2}{6\pi\lambda}, \quad (11)$$

where the prime represents derivative with respect to r. If $g_{\mu\nu}^{ABH}$ and c_s are taken as $\delta_{\mu\nu}$ and 1 respectively, the metric (8) reduces to the form (7) of the AdS-Schwarzschild spacetime. On the other hand, if we take $g_{\mu\nu}^{GR}$ and c_s to be $\eta_{\mu\nu}$ and 1 respectively, then the metric (8) returns to the metric given in (3).

C. Acoustic black holes from general relativistic fluids

To test the generality of the chaotic bound, we will also consider the acoustic metric in Schwarzschild spacetime. Starting from the hydrodynamics, we consider u_μ, ρ, p, n, s are the three-velocity, energy density, pressure, particle number density and entropy density of the fluid respectively. From the continuity equation,

$$\partial_\mu\left(\sqrt{-g^{GR}}nu^\mu\right) = 0, \quad (12)$$

where $u_\mu u^\mu = g_{\mu\nu}^{GR}u^\mu u^\nu = -1$ and the velocity potential equation,

$$\mathfrak{w}u_\mu = -\partial_\mu \psi, \qquad (13)$$

and the specific enthalpy $\mathfrak{w} = (p + \rho)/n$. By making the acoustic perturbations on u^μ, $\mathfrak{w}$, n, ψ,

$$u^\mu \to u^\mu + \delta u^\mu, \qquad \mathfrak{w} \to \mathfrak{w} + \delta\mathfrak{w},$$
$$n \to n + \delta n, \qquad \psi \to \psi + \delta\psi, \qquad (14)$$

we can obtain the wave equation,

$$\partial_\mu \left\{ \sqrt{-g^{GR}} \frac{n}{\mathfrak{w}} \left[g_{GR}^{\mu\nu} + \left(1 - \frac{\mathfrak{w}}{n}\frac{\partial n}{\partial \mathfrak{w}}\right) u^\nu u^\mu \right] \right\} \partial_\nu \delta\psi = 0. \qquad (15)$$

By some transformations and taking $c_s^2 = \frac{n}{\mathfrak{w}}\frac{\partial \mathfrak{w}}{\partial n}\big|_{s/n}$, the form of metric can be recast as (see [17–19] for details)

$$ds^2 = \tilde{\mathbb{G}}_{\mu\nu} dx^\mu dx^\nu = [g_{\mu\nu}^{GR} + (1 - c_s^2)u_\mu u_\nu] dx^\mu dx^\nu. \qquad (16)$$

In fact, there is a common coefficient factor in front of each metric component, which is related to the speed of sound, the density of fluid particles, the density of fluid energy and the pressure of the fluid. In order to simplify the calculation, we set this coefficient be 1. There are some differences between formula (6) and formula (16). The former is obtained from the Gross-Pitaevskii theory, while the latter is obtained from fluid mechanics.

III. FALLING INTO THE (2 + 1)-DIMENSIONAL ACOUSTIC BLACK HOLES IN MINKOWSKI SPACETIME: VORTEX MOTION AND CHAOS

In this section, we study the momentum growth of an infalling vortex toward an acoustic black hole. Unstable orbits and the momentum growth can be quantified by their Lyapunov exponents [23]. We use Lyapunov exponent to describe the motion of a vortex near the acoustic black hole. It was proposed that vortices can behave as relativistic particles with their dynamics governed by the fluid metric [24,25] and their stability ensured by a topological number. Vortices with mass m_0 given by the Einstein's relation $E = m_0 c^2$ [26,27] cannot propagate at velocities faster than the sound speed. Let us consider a vortex with mass $m_0 = 1$ freely falling into the acoustic black hole along the radial axis. The acoustic metric is given in Eq. (3). The action of the geodesic motion of the infalling vortex is [28]

$$S = -\int \sqrt{-g_{\alpha\beta}\mathrm{u}^\alpha \mathrm{u}^\beta} d\tau, \qquad (17)$$

where $\mathrm{u}^\alpha = dx^\alpha/d\tau$ is tangent to the world line and x^α is the spacetime coordinate, τ is an arbitrary parameter of the vortex world line. The equation of motion from the above action is

$$\dot{\mathrm{u}}^\mu + \Gamma_{\alpha\beta}^\mu \mathrm{u}^\alpha \mathrm{u}^\beta - \frac{\dot{\eta}\mathrm{u}^\mu}{2\eta} = 0, \qquad (18)$$

where $\eta = -g_{\mu\nu}^{ABH}\mathrm{u}^\mu\mathrm{u}^\nu > 0$ and the dot represents the derivative with respect to τ. Note that the acoustic black hole metric in general does not satisfy the Einstein equation. The canonical momentum can be obtained by

$$p_\alpha = \frac{\delta S}{\delta \mathrm{u}^\alpha} = \frac{g_{\alpha\beta}\mathrm{u}^\beta}{\sqrt{-g_{\mu\nu}\mathrm{u}^\mu\mathrm{u}^\nu}}. \qquad (19)$$

We choose the gauge $\tau = t$ and take the ansatz $r = r(t)$, $\phi = $ constant. Then, Eqs. (18) and (19) reduce to

$$\dot{r} = -\left(-g^{rr}g_{tt} - \frac{g^{rr}g_{tt}^2}{A^2}\right)^{1/2}, \qquad (20)$$

$$p_r = (-A^2 g^{tt}g_{rr} - g_{rr})^{1/2}, \qquad (21)$$

where $\dot{r} < 0$ means the vortex falls into the acoustic black hole and $A = \sqrt{g_{tt}^2/\eta} > 0$ is an integral constant. We substitute Eq. (3) into (20)–(21) and obtain

$$\dot{r} = -\left(f^2 - \frac{f^3}{A^2}\right)^{1/2}, \qquad (22)$$

$$p_r = (A^2 f^{-2} - f^{-1})^{1/2}. \qquad (23)$$

We evaluate the growth rate of the momentum in the Rindler coordinate [29,30]. Since $d\rho/dr \sim 1/\sqrt{f}$, the Rindler momentum p_ρ near the acoustic horizon is given by

$$p_\rho \sim \sqrt{f}p_r \sim (A^2 f^{-1} - 1)^{1/2}. \qquad (24)$$

We can find $(r - \lambda) \propto e^{-4\pi Tt}$ in Eq. (22) near the acoustic black hole horizon, where $T = 1/(2\pi\lambda)$ is the Hawking temperature of the acoustic black hole. Near the acoustic horizon, the radial momentum p_ρ can be approximated as

$$p_\rho \propto (r - \lambda)^{-1/2} \sim e^{2\pi Tt}. \qquad (25)$$

We then obtain $p_\rho \sim e^{2\pi Tt}$. Therefore, the growth of the radial momentum near the acoustic horizon is described by the Lyapunov exponent $\Lambda_{\mathrm{Lyapunov}}$,

$$\Lambda_{\mathrm{Lyapunov}} = 2\pi T. \qquad (26)$$

It is interesting to note that the chaos bound is satisfied by the momentum growth of the "test" particle in the geometry of acoustic black holes. This shows that acoustic black holes are similar to the real black hole, which provides the possibility for the experimental simulation of the chaotic behavior near the black hole horizon.

IV. VORTEX MOTION AND CHAOS FOR ACOUSTIC BLACK HOLES IN CURVED SPACETIME

In this section we further consider vortex motion for acoustic black holes in curved spacetime. From the field theory and fluid mechanics, we will consider the motion of vortices as probe particles falling along the radial direction in Schwarzschild-AdS and Schwarzschild space-time respectively, so as to further test whether the momentum growth chaos bound to the falling particles in the bulk are still satisfied in the curved space-time background.

A. Acoustic black holes from Gross-Pitaevskii equation

In a Schwarzschild-AdS spacetime, through the Hadamard product, we consider that the metric (8) of the acoustic black hole in the curved space-time of $(2+1)$-dimensional Schwarzschild-AdS background.

Similarly, the action in curved spacetime is considered as

$$S = -\int \sqrt{-\mathcal{G}_{\alpha\beta}u^\alpha u^\beta} d\tau. \qquad (27)$$

We can obtain the radial momentum,

$$\dot{r} = -\left(\frac{f_{ABH}^2 f_{GR}^2}{3} - \frac{f_{ABH}^3 f_{GR}^3}{9\mathcal{A}^2}\right)^{1/2}, \qquad (28)$$

$$p_r = \mathcal{A}\left(3f_{ABH}^{-2}f_{GR}^{-2} - \frac{f_{ABH}^{-1}f_{GR}^{-1}}{\mathcal{A}^2}\right)^{1/2}, \qquad (29)$$

where $\mathcal{A} = \sqrt{\mathcal{G}_{tt}^2/\eta_1} > 0$ is the integral constant with the timelike condition $\eta_1 = -\mathcal{G}_{\mu\nu}u^\mu u^\nu > 0$.

Since $d\rho/dr = 1/\sqrt{f_{ABH}f_{GR}}$, the Rindler momentum p_ρ is

$$p_\rho = \left(\frac{3\mathcal{A}^2}{f_{ABH}f_{GR}} - 1\right)^{1/2}. \qquad (30)$$

Near the acoustic horizon, the Rindler momentum p_ρ can be approximated as

$$p_\rho \approx \left[\frac{3\sqrt{3}\mathcal{A}^2}{2(3\lambda - \sqrt{3}r_0)(r - \sqrt{3}\lambda)}\right]^{1/2} \sim \left(r - \sqrt{3}\lambda\right)^{-1/2}. \qquad (31)$$

By calculating the expression (28), we can obtain $(r - \sqrt{3}\lambda) \propto e^{-4\pi Tt}$, where $T = \frac{3\lambda^2 - r_0^2}{6\pi\lambda}$. We can find that the Lyapunov exponent $\Lambda_{\text{Lyapunov}}$ of the stable acoustic black hole in AdS-Schwarzschild space-time (i.e., the temperature T is a constant at the acoustic horizon) is equal to $2\pi T$ and still satisfies the relation $\Lambda_{\text{Lyapunov}} = 2\pi T$. This is consistent with the results of pure acoustic black holes obtained in Eq. (26). It shows that for different types

of acoustic black holes, the growth of radial momentum still satisfies the chaotic bound.

B. Acoustic black holes from general relativistic fluids

From the perspective of fluid mechanics, in the $(2+1)$-dimensional Schwarzschild background, $u_\mu = (-1, -\frac{1}{f_0}(\frac{2M}{r})^{1/2}, 0)$, Eq. (16) is considered as

$$
\begin{aligned}
ds^2 &= \tilde{\mathbb{G}}_{\mu\nu}dx^\mu dx^\nu \\
&= \left(\frac{2}{3} - f_0\right)d\tilde{t}^2 + \frac{4\sqrt{2M}}{3f_0\sqrt{r}}dt dr \\
&\quad + \left(\frac{4M}{3f_0^2 r} + \frac{1}{f_0}\right)dr^2 + r^2 d\phi^2,
\end{aligned} \qquad (32)
$$

where M is the mass of the black hole and $f_0 = 1 - \frac{2M}{r}$. By considering the coordinate transformation $dt = d\tilde{t} + \frac{2\sqrt{2M}}{3f_0\sqrt{r}}dr$, we can obtain

$$
\begin{aligned}
ds^2 &= \mathbb{G}_{\mu\nu}dx^\mu dx^\nu \\
&= \left(\frac{2}{3} - f_0\right)dt^2 - \frac{3f_0 r + 4M - 2r}{2f_0 r - 3f_0^2 r}dr^2 + r^2 d\phi^2. \qquad (33)
\end{aligned}
$$

For a null hypersurface $\boldsymbol{F}(x^\mu) = 0$, it satisfies the definition,

$$\mathbb{G}^{\mu\nu}\frac{\partial \boldsymbol{F}}{\partial x^\mu}\frac{\partial \boldsymbol{F}}{\partial x^\nu} = 0. \qquad (34)$$

For steady-state spacetime, $\boldsymbol{F}$ should be time independent, and spacetime should be symmetric along ϕ direction, that is, $\boldsymbol{F}$ is a function of r. Therefore, the acoustic horizon can be calculated as $r = 6M$. And from the metric (32), we can find that the Hawking temperature of the acoustic balck hole is $T = \frac{1}{24\sqrt{3}\pi M}$.

Analogously, from the action $S = -\int \sqrt{-\mathbb{G}_{\alpha\beta}u^\alpha u^\beta} d\tau$, we obtained the radial coordinate change rate and radial momentum are respectively,

$$\dot{r} = -\left(-\frac{\mathbb{G}_{tt}}{\mathbb{G}_{rr}} - \frac{\mathbb{G}_{tt}^2}{\mathbb{A}^2 \mathbb{G}_{rr}}\right)^{1/2}, \qquad (35)$$

$$p_r = \left(-\frac{\mathbb{A}^2 \mathbb{G}_{rr}}{\mathbb{G}_{tt}} - \mathbb{G}_{rr}\right)^{1/2} = -\frac{\mathbb{A}\mathbb{G}_{rr}}{\mathbb{G}_{tt}}\dot{r}, \qquad (36)$$

where $\mathbb{A}$ is an integral constant and greater than 0. Through the approximate calculation near the acoustic horizon, we obtained $\dot{r} \sim (r - 6M) \sim e^{-4\pi Tt}$ from Eq. (35). The Rindler momentum can be expressed as

$$p_\rho = \mathbb{G}_{rr}^{-1/2}p_r = -\frac{\mathbb{A}\mathbb{G}_{rr}^{1/2}}{\mathbb{G}_{tt}}\dot{r} \sim e^{2\pi Tt}, \qquad (37)$$

which shows the momentum growth bound still holds at the horizon.

This demonstrates that not only near the real black hole, but also for the general nonrotating acoustic black hole, the exponent of the momentum growth of the Rindler coordinate near the event horizon satisfy $\Lambda_{\text{Lyapunov}} \leq 2\pi T$.

V. VORTICES ORBITS

In the above two sections, we consider the momentum growth of the vortex as the test particle near the horizon of the acoustic black hole. In this section, we will study the trajectory of vortices near acoustic black holes. We will consider the falling trajectory of vortices with different initial energy and angular momentum, and numerically calculate the radial momentum of particles growth with time t.

A. Effective potential

Since the metric (2) is independent of t and ϕ, the quantities $\boldsymbol{\xi} \cdot \mathbf{u}$ and $\boldsymbol{\eta} \cdot \mathbf{u}$ are conserved, where $\mathbf{u}$ is the "three-velocity" of the vortex, $\xi^\alpha = (1, 0, 0)$ and $\eta^\alpha = (0, 0, 1)$ are killing vectors. The conserved energy per unit of static mass is [31,32]

$$\epsilon = -\boldsymbol{\xi} \cdot \mathbf{u} = (1 - v^2)\frac{dt}{d\tau}. \quad (38)$$

The conservation angular momentum per unit of rest mass is

$$l = \boldsymbol{\eta} \cdot \mathbf{u} = r^2 \frac{d\phi}{d\tau}. \quad (39)$$

The "three-velocity" vectors satisfy the relation,

$$\mathbf{u} \cdot \mathbf{u} = g_{\alpha\beta}u^\alpha u^\beta = -1. \quad (40)$$

Substituting (2) into (40), we arrive at

$$-(1 - v^2)(u^t)^2 + (1 - v^2)^{-1}(u^r)^2 + r^2(u^\phi)^2 = -1. \quad (41)$$

Writing $u^t = dt/d\tau$, $u^r = dr/d\tau$, and $u^\phi = d\phi/d\tau$, and substituting (38) and (39) into (41) to eliminate $dt/d\tau$ and $d\phi/d\tau$, we obtain

$$-(1 - v^2)^{-1}\epsilon^2 + (1 - v^2)^{-1}\left(\frac{dr}{d\tau}\right)^2 + \frac{l^2}{r^2} = -1. \quad (42)$$

The square of the conservation energy per unit of rest mass can be obtained as

$$\epsilon^2 = \left(\frac{dr}{d\tau}\right)^2 + \left(\frac{l^2}{r^2} + 1\right)(1 - v^2). \quad (43)$$

By defining the effective energy [33–35],

$$\varepsilon \equiv \frac{\epsilon^2 - 1}{2} = \frac{1}{2}\left(\frac{dr}{d\tau}\right)^2 + V_{\text{eff}}(r), \quad (44)$$

where the effective potential is

$$V_{\text{eff}}(r) = \frac{1}{2}\left(-v^2 + \frac{l^2}{r^2} - v^2\frac{l^2}{r^2}\right), \quad (45)$$

and $v = -\lambda/r$. We obtain the expression of the effective potential,

$$V_{\text{eff}}(r) = \frac{1}{2r^4}[(l^2 - \lambda^2)r^2 - \lambda^2 l^2]. \quad (46)$$

For a concrete acoustic black hole, we know that λ is a positive constant, and $l^2 \geq 0$. If the first order derivative of the effective potential $V'_{\text{eff}}(r) = 0$, the critical radius satisfies $r_*^2 = \frac{2\lambda^2 l^2}{l^2 - \lambda^2}$. When $l^2 > \lambda^2$, we can obtain $r_* = \frac{\sqrt{2}\lambda l}{\sqrt{l^2 - \lambda^2}}$, and the second derivative of the effective potential, $V''_{\text{eff}}(r_*) = -\frac{4\lambda^2 l^2}{r_*^6} < 0$, which means that r_* is the radius of the unstable orbit. When $l^2 \leq \lambda^2$, we can find $V'_{\text{eff}}(r) > 0$ and $V''_{\text{eff}}(r) < 0$, which means that the effective potential $V_{\text{eff}}(r)$ increases with the increase of r and there is no stable orbit [36,37].

As shown in Fig. 2, the effective potential energy $V_{\text{eff}}(r)$ does not have a minimum value, so there is no stable circular orbit for the acoustic black hole of this type. Figure 3 shows four types orbits for values of l and e. As shown in the first row in Fig. 3, when the conservation angular momentum of the test particle is 0, the radial potential function of the particle increases monotonically with r and the particle always falls straight into the acoustic black hole. The second and the third row in Fig. 3 with the same potential but has different value of e ($l/\lambda = 1.4$), which means the different orbits. The value of e^2/λ^2 is 1.16, and the vortex will fall into the acoustic black hole as shown in the second row in Fig. 3. When the value of $e^2/\lambda^2 = 1.08$, the vortex will approach but escape the acoustic black hole as shown in the third row in Fig. 3, which also demonstrates the critical unstable orbit with the ratio of e^2/λ^2 is about 1.12.
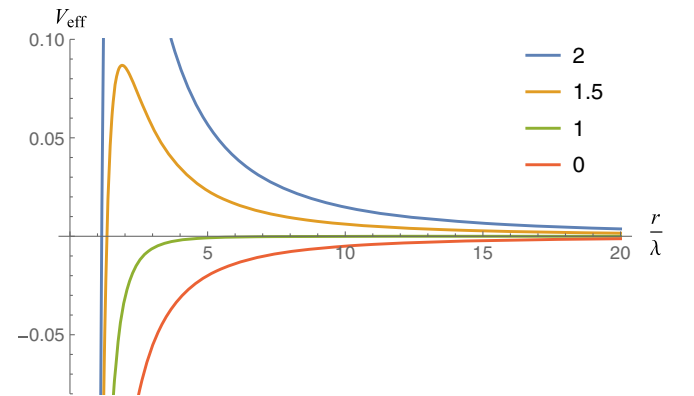

FIG. 2. We plot the effective potential V_{eff} as a function of r/λ by setting $l/\lambda = 0, 1, 1.5, 2$. It can be seen from the figure that there is no minimum point for the effective potential, that is, there is no stable circular orbit for the vortex.
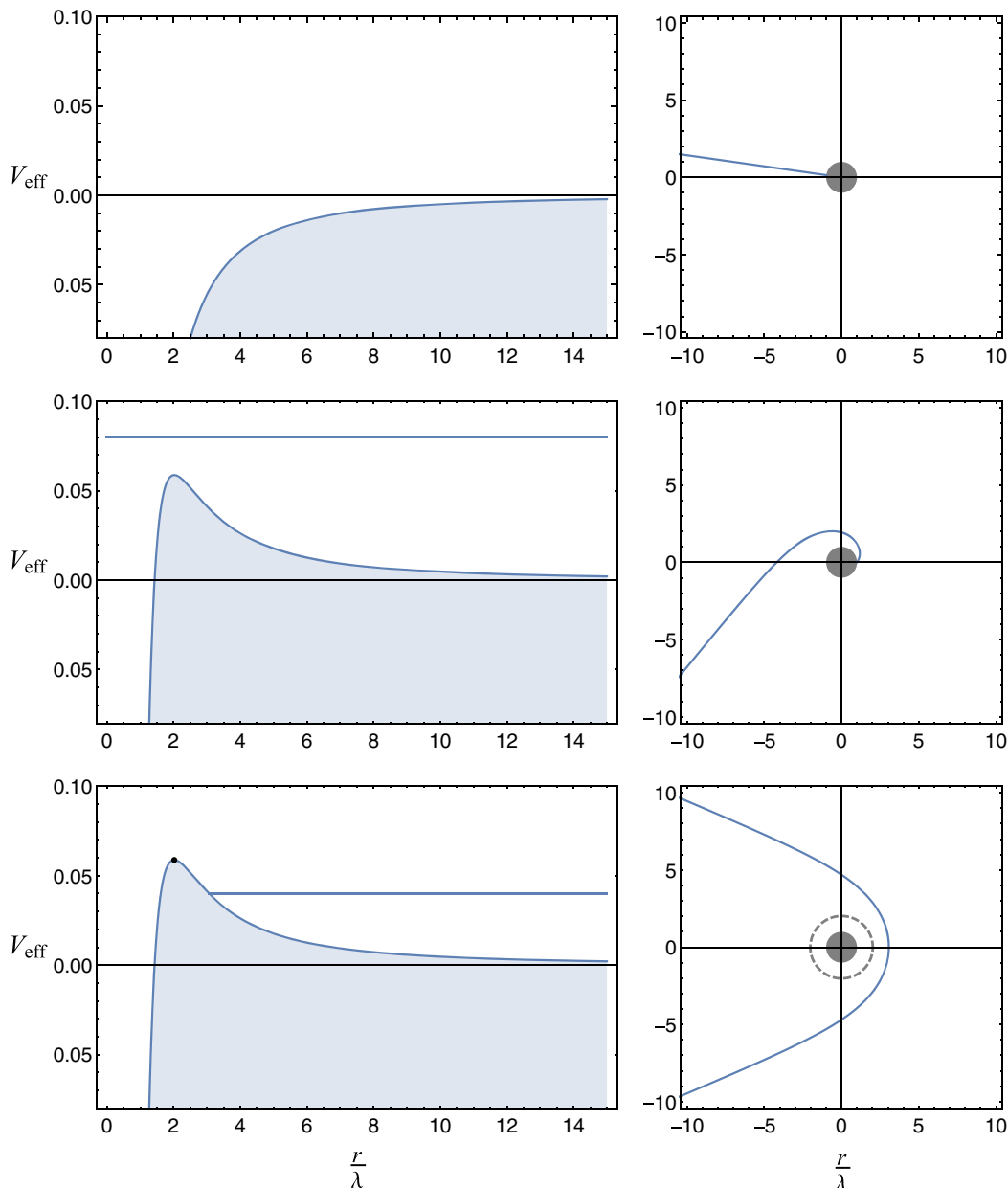
FIG. 3. From the first row, it can be seen that when $l = 0$, the potential function increases monotonically with r, and the vortex always falls straight into the acoustic black hole. The case of $l^2 < \lambda^2$ is similar. The value l/λ is 1.4 in other parts. For $l^2 > \lambda^2$, if the vortex energy is large enough, it will fall into the acoustic black hole, as shown in the second row. If the vortex energy is low, when the vortex is near the acoustic black hole, it will escape from the acoustic black hole, as shown in the third pair of pictures, where the dotted line on the right is the position of unstable orbit, corresponding to the maximum potential energy in the left figure.

B. Radial infalling orbit

From the effective energy equation (44) and the effective potential equation (45), we can study the radial motion of the vortices. From the Eq. (44) with $\epsilon = 1$ and $l = 0$, there is

$$0 = \frac{1}{2}\left(\frac{dr}{d\tau}\right)^2 - \frac{1}{2}v^2 = \frac{1}{2}\left(\frac{dr}{d\tau}\right)^2 - \frac{1}{2}\frac{\lambda^2}{r^2}, \quad (47)$$

where r decreases with the increase of τ in which the "three-velocity" component is given by $dr/d\tau = v < 0$. Taken together with the time component $dt/d\tau$ given by Eq. (38), the "three-velocity" is

$$u^\alpha = [(1-v^2)^{-1}, v, 0] = \left[\left(1 - \frac{\lambda^2}{r^2}\right)^{-1}, -\frac{\lambda}{r}, 0\right]. \quad (48)$$

Considering that $\lambda > 0$, we take a negative sign. Rewritten (47) in the form,

$$\frac{1}{v}dr = d\tau, \tag{49}$$

$$-\left(\frac{\lambda^2}{r^2}\right)^{-\frac{1}{2}}dr = -\frac{r}{\lambda}dr = d\tau, \tag{50}$$

the integral result is

$$r(\tau) = [-2\lambda(\tau - \tau_*)]^{1/2} = (2\lambda)^{1/2}(\tau_* - \tau)^{1/2}, \tag{51}$$

where τ_* is an integral constant. Computing dt/dr from Eq. (38) with $\epsilon = 1$ and Eq. (47), we obtain

$$\frac{dt}{dr} = (1 - v^2)^{-1}v^{-1} = -\left(1 - \frac{\lambda^2}{r^2}\right)^{-1}\frac{r}{\lambda} = -\frac{r^3}{\lambda(r^2 - \lambda^2)}. \tag{52}$$

After integration, we have

$$t = \int (1 - v^2)^{-1}v^{-1}dr = t_* - \frac{r^2 + \lambda^2 \ln(r^2 - \lambda^2)}{2\lambda}, \tag{53}$$

where t_* is another integral constant. From (53), when $r \to \infty, t \to -\infty$, the vortex is falling from infinity. From Eq. (51) we can see that for any fixed r_1 value outside the horizon, it takes only a finite amount of proper time τ to reach $r_2 = \lambda$, while Eq. (53) shows that it takes an infinite quantity of coordinate time t. This is just a sign that the coordinates are flawed at $r = \lambda$. This shows that for the falling object A itself, the time from r_1 to r_2 is limited. For the observer B with fixed coordinates, he observed that A keeps approaching the horizon r_2. The observation here refers to the sound waves received by B from A. Replacing ω_∞, v_∞ with ω_{r_1}, v_{r_1} and replacing ω_*, v_* with ω_{r_2}, v_{r_2} in (A9), we then obtain $\omega_{r_1} = 0$. The sound waves from r_2 are infinitely redshift.[1] B receives A's sound frequency is becoming lower and lower, and finally A's voice seems to solidify at r_2.

We can also use formula (53) to verify the relationship between the radial momentum of vortex falling and time. From Eqs. (20), (21) and (24), we obtain $p_\rho \sim -\dot{r}/(\sqrt{f\eta})$. Further considered the formula (53), the relationship between p_ρ and t can be obtained. Setting $t_* = 0, \lambda = 1$, thus $2\pi T = 1$, and r near the horizon, we obtain $p_\rho \sim e^{0.9997t}$ as shown in Fig. 4. Notice that t_* only shifts the $p_\rho - t$ curve horizontally, it does not affect the exponential relationship between $p_\rho - t$. After careful verifications, we observe that as r approaches the horizon λ, $\frac{\ln p_\rho}{t}$ approaches $2\pi T$. This shows that the acoustic black hole still satisfies the chaos bound of the momentum growth, which may

---

[1]For the discussions on redshift of sound wave propagation, one may refer to the Appendix.
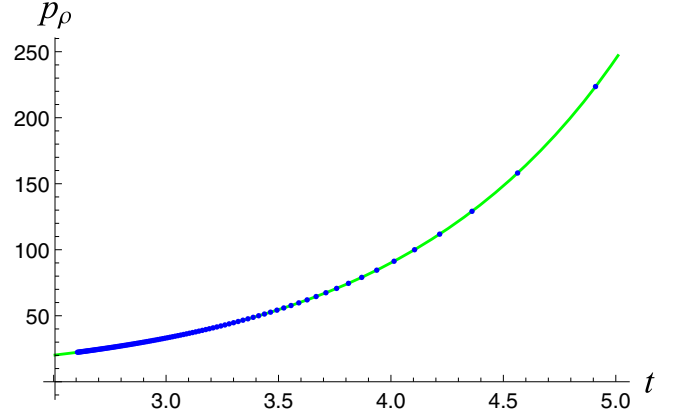

FIG. 4. In the figure, the blue points are the values of p_ρ and t calculated by numerical solution, and the green line is the curve of exponential fitting of data. Setting $t_* = 0, \lambda = 1$, which means $2\pi T = 1$, and r near the horizon, the fitting result is $p_\rho \sim e^{0.9997t}$.

provide a theoretical basis for simulating the chaotic behavior of particles falling into the real black hole.

VI. SOUND WAVE ORBITS

In addition to the computation of the Lyapunov exponent, the stability of the sound wave orbits and the Shapiro time delay of sound propagation near acoustic black hole deserve further investigations. In what follows, we first calculate the deflection angle and then the time delay of sound wave propagation in a $(2 + 1)$-dimensional acoustic black hole background in flat spacetime.

A. Sound wave deflection

The calculation of sound wave orbits in the acoustic geometry is analogous to the calculation of vortices orbits, but with some important differences. For vortices, the unstable critical orbit does not necessarily exist, and the critical radius of the orbit is related to angular momentum, while the unstable critical radius of the acoustic wave is fixed and smaller. The world line of sound waves can be described by the coordinates x^α as function of a family of affine parameters χ. The null vector $u^\alpha = dx^\alpha/d\chi$ is tangent to the world line. Since the acoustic metric (2) is independent of t and ϕ, the quantities,

$$\epsilon = (1 - v^2)\frac{dt}{d\chi}, \tag{54}$$

$$l = r^2\sin^2\theta\frac{d\phi}{d\chi}, \tag{55}$$

are conserved along sound wave orbits. If the normalization of χ is chosen so that **u** coincides with the momentum **p** of a beam of sound wave moving along the null geodesic, then ϵ and l are the sound wave's energy and angular momentum

at infinity. Since $\mathbf{u} \cdot \mathbf{u} = g_{\alpha\beta} \frac{dx^\alpha}{d\chi} \frac{dx^\beta}{d\chi} = 0$, considering the equatorial plane condition $\theta = \pi/2$, we have

$$-(1 - v^2)(u^t)^2 + (1 - v^2)^{-1}(u^r)^2 + r^2(u^\phi)^2 = 0. \quad (56)$$

Utilizing Eqs. (54) and (55), we have

$$-(1 - v^2)^{-1}\epsilon^2 + (1 - v^2)^{-1}\left(\frac{dr}{d\chi}\right)^2 + \frac{l^2}{r^2} = 0. \quad (57)$$

Multiplied by $(1 - v^2)/l^2$, it can be written as

$$\frac{1}{b^2} = \frac{1}{l^2}\left(\frac{dr}{d\chi}\right)^2 + W_{\text{eff}}, \quad (58)$$

therein

$$b^2 = l^2/\epsilon^2, \quad (59)$$

and

$$W_{\text{eff}} = \frac{1}{r^2}(1 - v^2). \quad (60)$$

In the equatorial plane,

$$x = r\cos\phi, \qquad y = r\sin\phi, \quad (61)$$

suppose a beam of sound wave moves parallel to the x-axis, and the distance from the x-axis is d, as shown in Fig. 5. At a distance from the source of an acoustic black hole, the sound wave moves in a straight line. For $r \gg \lambda$, the quantity b is

$$b = \left|\frac{l}{\epsilon}\right| = \frac{r^2}{1 - v^2}\frac{d\phi}{dt} \approx r^2\frac{d\phi}{dt}. \quad (62)$$

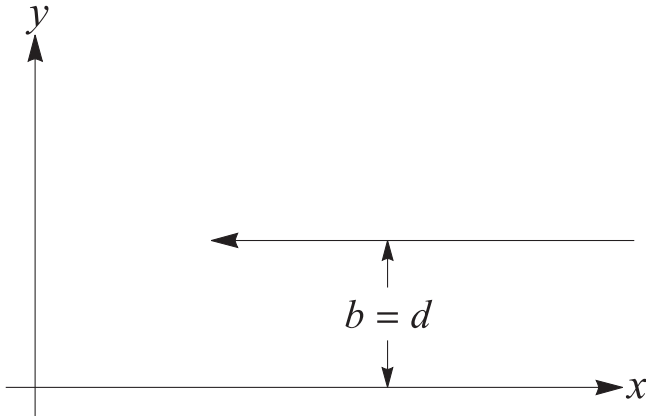For very large r there are $\phi \approx d/r$, and $dr/dt \approx -1$, it becomes

y

$b = d$

x

$$\frac{d\phi}{dt} = \frac{d\phi}{dr}\frac{dr}{dt} = \frac{d}{r^2}. \quad (63)$$

Therefore,

$$b = d. \quad (64)$$

This shows that the constant b is a parameter of sound waves ray reaching infinity and is defined to be positive. Figure 6 shows W_{eff} as a function of r on the left. It goes to zero at large r, and it has a maximum at $r = \sqrt{2}\lambda$. If $b = 2\lambda$, the circular orbit of the sound wave at the maximum $r = \sqrt{2}\lambda$. The maximum is

$$W_{\text{eff}}(\sqrt{2}\lambda) = \frac{1}{4\lambda^2}. \quad (65)$$

If $b^2 = 4\lambda^2$, it can be seen from formula (58) that the circular orbit of the sound wave is possible at radius $r = \sqrt{2}\lambda$ in the first pair of Fig. 6. However, the circular orbit is unstable. A small perturbation in b will result in orbit far away from the maximum. A stable sound wave circular orbit is impossible around the two-dimensional acoustic black hole in our model. The qualitative characteristics of other sound wave orbits depend on whether $1/b^2$ is greater than the maximum value of W_{eff}, as shown in Fig. 6. First of all, consider that orbits start at infinity, if $1/b^2 < 1/4\lambda^2$, the orbit will have a turning point and returns to infinity again,also as shown in the first line of Fig. 6. We will discuss the size of the deflection angle in detail in a minute. If $1/b^2 > 1/4\lambda^2$, the sound wave will fall all the way to the origin and be captured, as in the second line of Fig. 6. The angle of interest is the deflection angle $\delta\phi_{\text{def}}$, showed in Fig. 7. This angle shows a property of the shape of the sound wave orbit. This shape of a beam of sound wave can be calculated in the same way as the shape of a vortex orbit. Solve (55) for $d\phi/d\chi$, solve (58) for $dr/d\chi$, divide the second into the first, and then predigest using (59) and (60) to find

$$\frac{d\phi}{dr} = \pm\frac{1}{r^2}\left(\frac{1}{b^2} - W_{\text{eff}}\right)^{-\frac{1}{2}}. \quad (66)$$

The plus or minus sign indicates the direction of the orbit. When the sound wave comes in from infinity and comes back again, the total sweep angle $\Delta\phi$ is twice the sweep angle from the turning point $r = r_1$ to infinity. Therefore,

$$\Delta\phi = 2\int_{r_1}^\infty \frac{dr}{r^2}\left(\frac{1}{b^2} - \frac{1 - v^2}{r^2}\right)^{-\frac{1}{2}}. \quad (67)$$

The radius r_1 satisfies $1/b^2 = (1 - v^2)/r_1^2$; i.e., the radius where the bracket in the preceding expression vanishes. Set a new variable w defined by
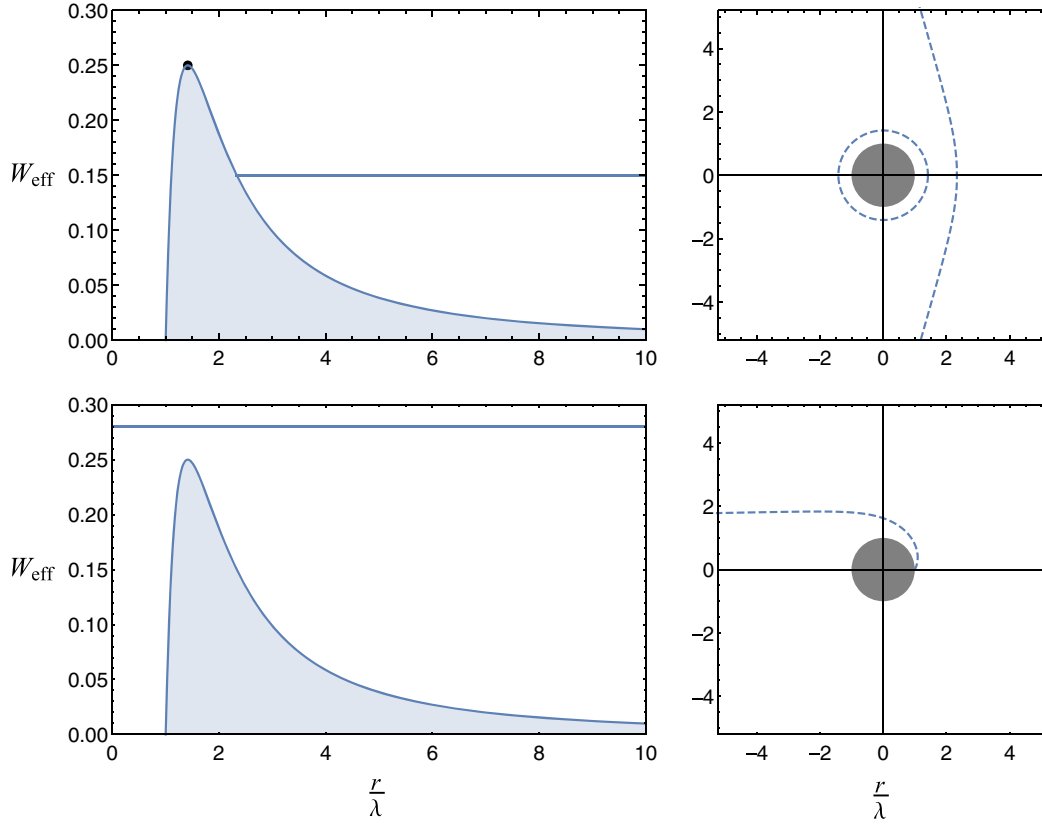
FIG. 6.   The picture shows three tracks corresponding to different b values. The relationship between potential W_{eff} and $1/b^2$ is shown in the left column. The effective potential of the acoustic black hole and the behavior of the sound wave passing through the acoustic black hole: when the beam of sound wave energy is equal to the maximum value of the effective potential of the acoustic black hole, it is a critical state; when the beam of sound wave energy is less than the height of the barrier, the sound wave does not fall into the acoustic black hole; when the beam of sound wave energy is greater than the barrier height, the sound wave will fall into the black hole.

$$r = \frac{b}{w}, \tag{68}$$

the expression of $\Delta\phi$ turns out to be

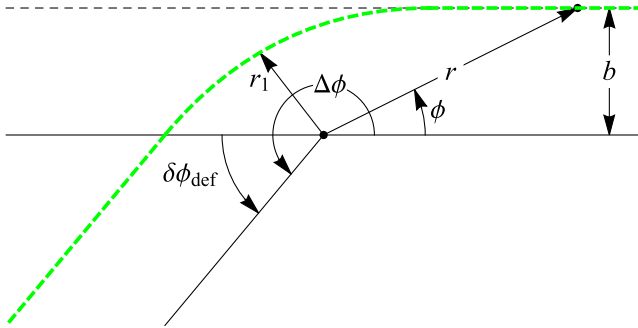$$\Delta\phi = 2 \int_0^{w_1} dw [1 - w^2(1 - v^2)]^{-\frac{1}{2}}, \tag{69}$$

FIG. 7.   In this figure, b is the linear distance from the black hole to the incident direction of the sound wave. A beam of sound wave coming from infinite distances pass through the vicinity of acoustic black holes and deflect in a direction of $\delta\phi_{def}$.

where $w_1 = b/r_1$ is the value of w at the turning point. For $v^2 = \lambda^2/r^2 = \lambda^2 w^2/b^2$, we have

$$\Delta\phi = 2 \int_0^{w_1} dw \left[1 - w^2\left(1 - \frac{\lambda^2}{r^2}\right)\right]^{-\frac{1}{2}}$$

$$= 2 \int_0^{w_1} dw \left[1 - w^2\left(1 - \frac{\lambda^2 w^2}{b^2}\right)\right]^{-\frac{1}{2}}. \tag{70}$$

When the value of v is much less than 1, i.e., r is much larger than λ and $\lambda w/b$ is far less than 1, we can recast Eq. (70) as

$$\Delta\phi = 2 \int_0^{w_1} dw \left(1 - \frac{\lambda^2 w^2}{b^2}\right)^{-\frac{1}{2}} \left[\left(1 - \frac{\lambda^2 w^2}{b^2}\right)^{-1} - w^2\right]^{-\frac{1}{2}}. \tag{71}$$

Expand the exponential term of $(1 - \lambda^2 w^2/b^2)$ as a power series,

$$\Delta\phi = 2 \int_0^{w_1} dw \frac{1 + 2\lambda^2 w^2/b^2}{(1 + \lambda^2 w^2/b^2 - w^2)^{\frac{1}{2}}} = \frac{\pi}{(1 - \lambda^2/b^2)^{\frac{3}{2}}}, \tag{72}$$

where w_1 is a root of the denominator in Eq. (72). For small λ/b, it becomes

$$\Delta\phi = \pi\left(1 + \frac{3}{2}\frac{\lambda^2}{b^2}\right). \tag{73}$$

Therefore, the deflection angle is

$$\delta\phi_{\text{def}} = \frac{3}{2}\frac{\lambda^2}{b^2}\pi. \tag{74}$$

Reinserted the factor of c_s (sound velocity), the above formula can be written as (b has dimensions of length)

$$\delta\phi_{\text{def}} = \frac{3}{2}\frac{c_s^2\lambda^2}{b^2}\pi, \tag{75}$$

for small $c_s\lambda/b$. This shows that the deflection angle of the sound wave is directly proportional to the square of the $c_s\lambda/b$.

B. Time delay of sound waves

Since the sound wave trajectory bends near the acoustic black hole, the path of sound wave transmission at the same two points becomes longer, as shown in Fig. 8. The quantities r_1, r_2, and r_3 are radii of the orbits of the closest point, reflector, and observer to the acoustic black hole, respectively. Thus, the time for the sound wave to travel back and forth between the observer and the reflector will

increase. According to Eq. (54) for $dt/d\chi$ and Eq. (58) for $dr/d\chi$, we can obtain

$$\frac{dt}{dr} = \pm\frac{1}{b}\left(1 - \frac{\lambda^2}{r^2}\right)^{-1}\left(\frac{1}{b^2} - W_{\text{eff}}\right)^{-\frac{1}{2}}, \tag{76}$$

where the positive sign is suitable for increasing radius, and the negative sign is suitable for decreasing radius. From the left of Fig. 8, we can see that the total time for sound wave travel forth and back between observer and reflector is

$$\Delta t_{\text{total}} = 2t(r_1, r_2) + 2t(r_1, r_3), \tag{77}$$

where the time required for a beam of sound wave moving from a radius of r_1 to a radius of r is

$$t(r_1, r) = \int_{r_1}^{r} dr \frac{1}{b}\left(1 - \frac{\lambda^2}{r^2}\right)^{-1}\left(\frac{1}{b^2} - W_{\text{eff}}\right)^{-\frac{1}{2}}, \tag{78}$$

among them,

$$b^2 = r_1^2\left(1 - \frac{\lambda^2}{r_1^2}\right)^{-1}, \qquad W_{\text{eff}} = \frac{1}{r^2}\left(1 - \frac{\lambda^2}{r^2}\right). \tag{79}$$

We consider λ/r as a small quantity, simplify and approximate the above formula, then
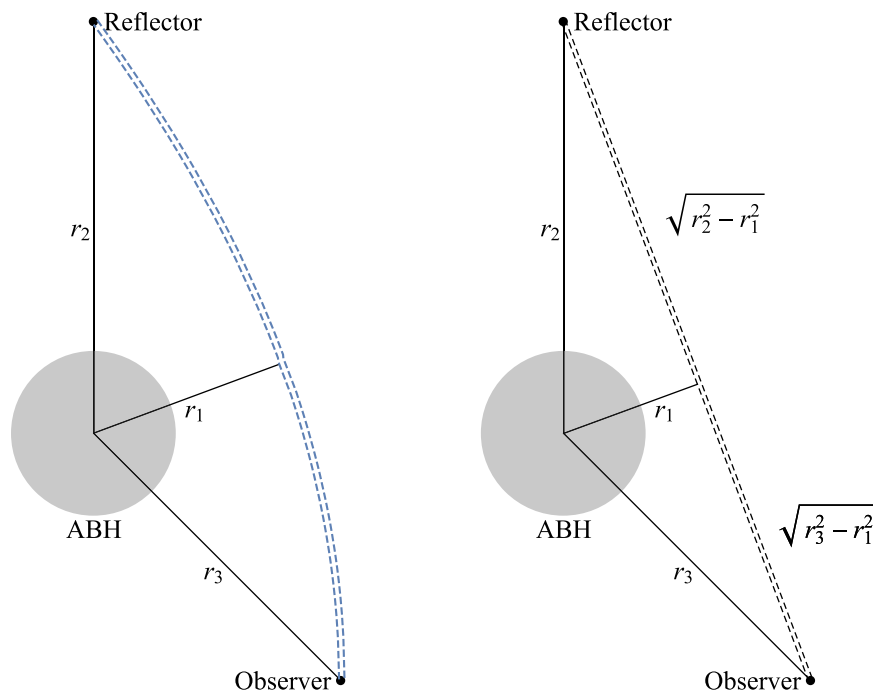

FIG. 8.   Sound waves bend by trajectories near acoustic black holes: the left figure shows the situation when the trajectory bends, while the right figure corresponds to the trajectory without bending. Obviously, when the trajectory bends, the trajectory becomes longer and the reflected signal is relatively delayed.

$$t(r_1, r) = \int_{r_1}^{r} dr \left(1 - \frac{\lambda^2}{r^2}\right)^{-\frac{3}{2}} \left(1 - \frac{r_1^2}{r^2}\right)^{-\frac{1}{2}}$$

$$\approx \int_{r_1}^{r} dr \left(1 + \frac{3\lambda^2}{2r^2}\right) \left(1 - \frac{r_1^2}{r^2}\right)^{-\frac{1}{2}}. \quad (80)$$

The integral can be evaluated as

$$t(r_1, r) = \sqrt{r^2 - r_1^2} + \frac{3\lambda^2}{2r_1} \left(\frac{\pi}{2} - \arctan\frac{r_1}{\sqrt{r^2 - r_1^2}}\right). \quad (81)$$

Thus,

$$\Delta t_{\text{total}} = \sqrt{r^2 - r_1^2} + \frac{3\lambda^2}{2r_1} \left(\frac{\pi}{2} - \arctan\frac{r_1}{\sqrt{r^2 - r_1^2}}\right). \quad (82)$$

Then the radar echo delay is

$$\Delta t_{\text{excess}} = \Delta t_{\text{total}} - 2\sqrt{r_2^2 - r_1^2} - 2\sqrt{r_3^2 - r_1^2}. \quad (83)$$

Considering $r_1/r_2 \ll 1, r_1/r_3 \ll 1$ and sound velocity c_s, we can recast (83) as

$$\Delta t_{\text{excess}} \approx \frac{3c_s^2\lambda^2}{r_1} \left(\pi - \frac{r_1}{r_2} - \frac{r_1}{r_3}\right) = 3c_s^2\lambda^2 \left(\frac{\pi}{r_1} - \frac{1}{r_2} - \frac{1}{r_3}\right). \quad (84)$$

We can see that the time delay is mostly related to λ. The larger the λ is, the more the time delay is. The parameter λ corresponds to the flow velocity around the acoustic black hole, which is equivalent to the mass of the black hole. Note that λ also corresponds to the radius of the horizon. Therefore, the time delay is closely related to the nature of the central acoustic black hole. Then, since π/r_1 is much larger than $1/r_2$ and $1/r_3$, this reflects that r_1 is the closest point to the acoustic black hole, which has a greater impact on the time delay effect. This can be understood as the closer to the acoustic black hole is, the more obvious the bending of the sound trajectory is, and the greater time delay effect is.

VII. DISCUSSION AND CONCLUSION

In summary, the geometry outside a $(2 + 1)$-dimensional acoustic black hole encodes interesting physics. For vortices falling into the acoustic black holes along the radial axis, the growth of the radial momentum near the horizon has the relation $p_r \sim e^{2\pi T t}$, signalizing the chaos behavior with the Lyapunov exponent $\Lambda_{\text{Lyapunov}} = 2\pi T$. In the case of the AdS-Schwarzschild background, the increase of the momentum near the horizon of acoustic black holes is $e^{2\pi T t}$. These are in agreement with the chaos bound proposed in [16]. The result is further confirmed from the numerical calculation of the radial infalling orbit of the

vortex. It is a little bit surprising that it saturates the chaos bound since that acoustic black holes can only simulate the kinetic aspects of real black holes, but it does not satisfy the Einstein equation. It would be interesting to verify this point experimentally.

Taking vortices as relativistic particles outside acoustic black holes, we calculated in detail the effective potential and found that there is no stable circular orbit for vortices. As the radial falling orbit is further considered, there is no orbital precession. Sound wave deflection and sound wave time delay are further investigated. The results show that the deflection angle of sound waves is inversely proportional to the square of the distance to the acoustic black hole. The time delay of sound waves passing through the vicinity of the acoustic black hole has the greatest correlation with the distance r_2 when the sound wave trajectory is closest to the acoustic black hole. It is inversely proportional to the initial distance r_1 and the final distance r_3 and r_1. That is to say, the greater the r is, the less the effect on the time delay will be.

APPENDIX: ACOUSTIC REDSHIFT

Let us consider an observer who emits a sound signal from a fixed radius r_* near the acoustic black hole. The original signal has frequency ω_* as measured by this stationary observer. The sound signal is measured by another stationary observer (see Fig. 9), where its
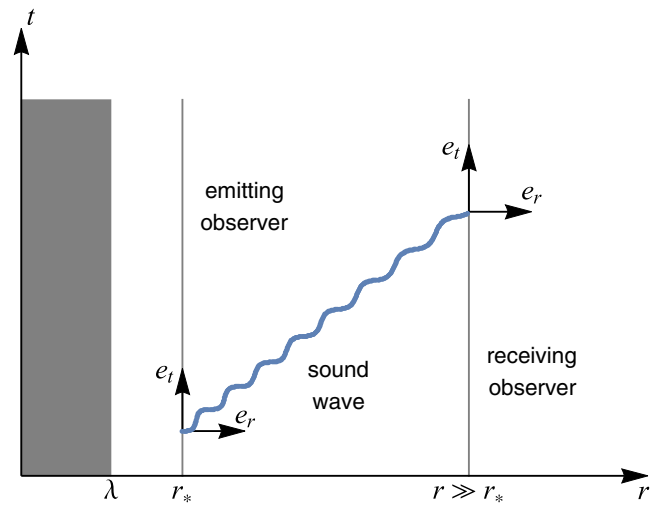

FIG. 9. A sound wave traveling from r_* to infinity, and the sound frequency measured by the receiver is lower than that of the sender.

frequency ω_∞ received by an observer at infinity is less than ω_*. The sound wave energy related to the viewer's "three-velocity" $\mathbf{u}_{\text{obs}}$ is [32]

$$E = -\mathbf{p} \cdot \mathbf{u}_{\text{obs}}. \tag{A1}$$

Since the energy of a beam of sound wave is $E = \hbar\omega$, $\hbar\omega = -\mathbf{p} \cdot \mathbf{u}_{\text{obs}}$ given the relationship between the observer's measured frequency and the "three-velocity" $\mathbf{u}_{\text{obs}}$. For a stationary observer, the spatial component u^j_{obs} of the "three-velocity" is zero ($j = r, \phi$). The time component $u^t_{\text{obs}}(r)$ at radius r for a stationary observer depend on the normalization condition,

$$\mathbf{u}_{\text{obs}}(r) \cdot \mathbf{u}_{\text{obs}}(r) = g_{\alpha\beta} u^\alpha_{\text{obs}}(r) u^\beta_{\text{obs}}(r) = -1. \tag{A2}$$

For static black hole, $\mathbf{u}^i_{\text{obs}}(r) = 0$, and this means

$$g_{tt}(r)[u^t_{\text{obs}}(r)]^2 = -1. \tag{A3}$$

In other words,

$$u^t_{\text{obs}}(r) = (1 - v^2)^{-\frac{1}{2}}. \tag{A4}$$

Thus, the time-component of the "three-velocity" is given by

$$u^t_{\text{obs}}(r) = [(1 - v^2)^{-\frac{1}{2}}, 0, 0] = (1 - v^2)^{-\frac{1}{2}} \xi^\alpha, \tag{A5}$$

where $\boldsymbol{\xi}$ is the Killing vector $\xi^\alpha = (1, 0, 0)$ corresponding to the fact that the metric is time-independent. Therefore, for a stationary observer at radius r, one has

$$\mathbf{u}_{\text{obs}}(r) = (1 - v^2)^{-\frac{1}{2}} \boldsymbol{\xi}. \tag{A6}$$

Using $\hbar\omega = -\mathbf{p} \cdot \mathbf{u}_{\text{obs}}$ in Eq. (A6), the frequencies of the sound wave measured by the stationary observer at radius r_* and infinite radius r_∞ are

$$\hbar\omega_* = (1 - v^2_*)^{-\frac{1}{2}} (-\boldsymbol{\xi} \cdot \mathbf{p})_{r_*}, \tag{A7}$$

$$\hbar\omega_\infty = (1 - v^2_\infty)^{-\frac{1}{2}} (-\boldsymbol{\xi} \cdot \mathbf{p})_{r_\infty}. \tag{A8}$$

The quantity $\boldsymbol{\xi} \cdot \mathbf{p}$ is conserved along the sound wave's geodesic. That is, $(-\boldsymbol{\xi} \cdot \mathbf{p})_{r_*} = (-\boldsymbol{\xi} \cdot \mathbf{p})_{r_\infty}$. Therefore, the relationship between the frequencies is

$$\omega_\infty = \omega_* \left(\frac{1 - v^2_*}{1 - v^2_\infty}\right)^{\frac{1}{2}} = \omega_* \left(\frac{1 - \frac{\lambda^2}{r^2_*}}{1 - \frac{\lambda^2}{r^2_\infty}}\right)^{\frac{1}{2}} = \omega_* \left(1 - \frac{\lambda^2}{r^2_*}\right)^{\frac{1}{2}}. \tag{A9}$$

In the $r \to \infty$ limit, the frequency is less than the frequency at r_* by a factor $(1 - \lambda^2/r^2_*)^{1/2}$. The sound wave should be influenced by the "gravitational" redshift of the acoustic metric. If the position r_* of the signal sender approaches the acoustic horizon infinitely, the frequency observed at infinity will be infinitely low.

[1] J. R. Nova, K. Golubkov, V. I. Kolobov, and J. Steinhauer, Observation of thermal Hawking radiation and its temperature in an analogue black hole, Nature (London) **569,** 688 (2019).

[2] J. Drori, Y. Rosenberg, D. Bermudez, Y. Silberberg, and U. Leonhardt, Observation of Stimulated Hawking Radiation in an Optical Analogue, Phys. Rev. Lett. **122,** 010404 (2019).

[3] W. G. Unruh, Experimental Black-Hole Evaporation, Phys. Rev. Lett. **46,** 1351 (1981).

[4] M. Visser, Acoustic black holes: Horizons, ergospheres, and Hawking radiation, Classical Quantum Gravity **15,** 1767 (1998).

[5] K. G. Zloshchastiev, Acoustic phase lenses in superfluid helium as models of composite spacetimes in general relativity: Classical and quantum features, Acta Phys. Pol. B **30,** 897 (1998), arXiv:gr-qc/9802060.

[6] X. H. Ge, M. Nakahara, S. J. Sin, Y. Tian, and S. F. Wu, Acoustic black holes in curved spacetime and the emergence of analogue Minkowski spacetime, Phys. Rev. D **99,** 104047 (2019).

[7] X. H. Ge, S. F. Wu, Y. Wang, G. H. Yang, and Y. G. Shen, Acoustic black holes from supercurrent tunneling, Int. J. Mod. Phys. D **21,** 1250038 (2012).

[8] X. H. Ge and S. J. Sin, Acoustic black holes for relativistic fluids, J. High Energy Phys. 06 (2010) 087.

[9] X. H. Ge, J. R. Sun, Y. L. Zhang, X. N. Wu, and Y. Tian, Holographic interpretation of acoustic black holes, Phys. Rev. D **92,** 084052 (2015).

[10] C. Barceló, S. Liberati, and M. Visser, Towards the observation of Hawking radiation in Bose-Einstein condensates, Int. J. Mod. Phys. A **18,** 3735 (2003).

[11] C. Yu and J. R. Sun, Note on acoustic black holes from black D3-brane, Int. J. Mod. Phys. D **28,** 1950095 (2019).

[12] R. Balbinot, A. Fabbri, R. A. Dudley, and P. R. Anderson, Particle production in the interiors of acoustic black holes, Phys. Rev. D **100,** 105021 (2019).

[13] E. Bittencourt, V. A. De Lorenci, R. Klippert, and L. S. Ruiz, Effective acoustic geometry for relativistic viscous fluids, Phys. Rev. D **98,** 064042 (2018).

[14] L. Susskind, Why do Things Fall?, arXiv:1802.01198.

[15] L. Susskind and Y. Zhao, Complexity and momentum, arXiv:2006.03019.

[16] J. Maldacena, S. H. Shenker, and D. Stanford, A bound on chaos, J. High Energy Phys. 08 (2016) 106.

[17] M. Visser and C. Molina-París, Acoustic geometry for general relativistic barotropic irrotational fluid flow, New J. Phys. **12,** 095014 (2010).

[18] N. Bilić, Relativistic acoustic geometry, Classical Quantum Gravity **16,** 3953 (1999).

[19] V. Moncrief, Stability of stationary, spherical accretion onto a Schwarzschild black hole, Astrophys. J. **235,** 1038 (1980).

[20] J. R. Sun and Y. Sun, On the emergence of gravitational dynamics from tensor networks, arXiv:1912.02070.

[21] B. Rezník, Origin of the thermal radiation in a solid-state analog of a black hole, Phys. Rev. D **62,** 044044 (2000).

[22] S. A. Hartnoll, Lectures on holographic methods for condensed matter physics, Classical Quantum Gravity **26,** 224002 (2009).

[23] N. J. Cornish and J. Levin, Lyapunov timescales and black hole binaries, Classical Quantum Gravity **20,** 1649 (2003).

[24] G. E. Volovik, *The Universe in a Helium Droplet* (Clarendon Press and Oxford University Press, Oxford, 2003).

[25] P. M. Zhang, L. M. Cao, Y. S. Duan, and C. K. Zhong, Transverse force on a moving vortex with the acoustic geometry, Phys. Lett. A **326,** 375 (2004).

[26] V. N. Popov, Quantum vortices and phase transitions in Bose systems, Sov. Phys. JETP **37,** 341 (1973), http://jetp.ac.ru/cgi-bin/dn/e_037_02_0341.pdf.

[27] J. M. Duan, Mass of a vortex line in superfluid ^{4}He: Effects of gauge-symmetry breaking, Phys. Rev. B **49,** 12381 (1994).

[28] Z. Zhou and J. P. Wu, Particle motion and chaos, Adv. High Energy Phys. **2020,** 1670362 (2020).

[29] A. R. Brown, H. Gharibyan, A. Streicher, L. Susskind, L. Thorlacius, and Y. Zhao, Falling toward charged black holes, Phys. Rev. D **98,** 126016 (2018).

[30] S. P. Kim, Hawking radiation as quantum tunneling in Rindler coordinate, J. High Energy Phys. 11 (2007) 048.

[31] S. M. Carroll, *Spacetime and Geometry* (Addison-Wesley, San Francisco, 2004), pp. 205–222.

[32] J. B. Hartle, *Gravity: An Introduction to Einstein's General Relativity* (Addison-Wesley, Reading, MA, 2003), pp. 186–217.

[33] B. Carter, Global structure of the Kerr family of gravitational fields, Phys. Rev. **174,** 1559 (1968).

[34] J. M. Bardeen, W. H. Press, and S. A. Teukolsky, Rotating black hole: Locally nonrotating frames, energy extraction, and scalar synchrotron radiation, Astrophys. J. **178,** 347 (1972).

[35] F. de Felice, Angular momentum and separation constant in the Kerr metric, J. Phys. A **13,** 1701 (1980).

[36] L. Rezzolla and O. Zanotti, *Relativistic Hydrodynamics* (Oxford University Press, Oxford, 2013), pp. 52–58.

[37] C. W. Misner, K. S. Thorne, and J. A. Wheeler, *Gravitation* (Princeton University Press, Princeton, NJ, 2017), pp. 901–917.